University of Sistan and Baluchestan

Challenges in Nano and Micro Scale Science and Technology

Online ISSN: 2821 - 000X

Magnetic Hysteresis Loop Behavior of a Type of Tetra-Metallic Nanocomposite Prepared by Co-Precipitation

Fatemeh Mirbaluchzehi[1] | Abdol Mahmood Davarpanah[2]✉ | Sajad Rakhshani Aval[3]

1. Department of Physics, Faculty of Science, University of Sistan and Baluchestan, Zahedan, Iran.
2. Corresponding Author, Department of Physics, Faculty of Science, University of Sistan and Baluchestan, Zahedan, Iran, Email: a.m.davarpanah@phys.us.ac.ir
3. Department of Chemistry, Faculty of Science, University of Sistan and Baluchestan, Zahedan, Iran.

Article Info

Article type:
Research Article

Keywords:
Coprecipitation,
Magnetization,
Magnesium,
Ni-Mg-Co Ferrites,
Structural,
Tetra Metalic,
VSM

ABSTRACT

Nanoparticles unique chemical and physical properties signifiicantly differentiate them from their bulk and macroscopic counterparts. Their small size and specific surface area contribute to these differences. Nickel-magnesium-cobalt ferrite is a well-known spinel ferrite magnetic material recognized for excellent performance at high frequencies. It is a novel composite material formed by incorporating a specific amount of magnesium into the nickel-cobalt ferrite matrix, paving the way for further research into new combinations Nickel-iron-cobalt alloys are among the most significant magnetic metals, exhibiting significant ferromagnetism at temperatures above room temperature (RT). In this study, nickel-cobalt-magnesium-iron nanoparticles were synthesized using the coprecipitation method. The initial raw materials including metal nitrates, sodium hydroxide, and citric acid, were used for the occurrence of the reaction. Magnesium was substituted for nickel in the nickel-cobalt ferrite powders for a short duration. The resulting materials were analyzed using X-ray Diffraction (XRD), Scanning Electron Microscope (SEM), Fourier Transform Infrared (FTIR), and Vibrating Sample Magnetometry (VSM). The magnesium substitution influenced the particle size and magnetic properties of $Mg_xNi_{1-x}Co_{0.5}Fe_2O_4$ nanoparticles. The average size of the crystallites increased with the addition of magnesium while the lattice constant remained stable ranging from 8.375 to 8.397 nm. All samples exhibited a simple cubic crystal (SC) structure with a cauliflower-like morphology. According to the VSM results, the hysteresis loops indicate that as magnesium is added and nickel is reduced in the samples, both the Saturation Magnetization (M_s) and Remanent Magnetization (M_r) decreased. Adding magnesium and reducing nickel in the samples decreased the saturation magnetization (M_S) from 3.19 emu/g to 0.12 emu/g while the residual magnetization (M_r) decreased from 0.54 to 4.32×10^{-3} emu/g. Samples M01, M02, and M03 displayed ferromagnetic properties, whereas sample M04 exhibited characteristics similar to paramagnetism.

INTRODUCTION

In recent years, magnetic nanocomposites of metal oxides, particularly spinel ferrite, have emerged as a significant class of magnetic materials with diverse applications. Due to their unique properties, they occupy an important position in science and engineering [1]. These magnetic oxide nano-metals are extensively utilized in various fields, including magnetic recording [2], magnetic separation [3], ferrofluids [4], magnetic resonance imaging [5], biomedicine [6], catalysis [7], gas sensors [8], high – quality ceramics [9], and superparamagnetic materials [10]. Nickel-magnesium-cobalt ferrites are particularly valued for good chemical stability [11], high magnetic anisotropy [12], moderate magnetization [13], and significant mechanical hardness [14]. As a result, they find applications in information storage [15], electromechanical structures [16] and biomedicine [17].

This study aims to experimentally investigate the structural and magnetic properties of nickel-magnesium-cobalt-ferrite ($Mg_xNi_{1-x}Co_{0.5}Fe_2O_4$) nanoparticles prepared via the coprecipitation method.

How to Cite this paper: Mirbaluchzehi F, Davarpanah AM, Rakhshani Aval S. Magnetic Hysteresis Loop Behavior of a Type of Tetra-Metallic Nanocomposite Prepared by Co-Precipitation. *Challenges in Nano and Micro Scale Science and Technology*. 2023; 11(1): 25-30. DOI: 10.22111/cnmst.2024.49311.1251

© Mirbaluchzehi F, Davarpanah AM, Rakhshani Aval S. Publisher: University of Sistan and Baluchestan.

DOI: 10.22111/cnmst.2024.49311.1251

Motivation for Developing Ni-Mg-Co Ferrite Nanoparticles via the Coprecipitation Process, Versatile Magnetic Properties, Cost-Effective Synthesis, Scalability and Reproducibility, Enhanced Functionalization Potential, Environmental Considerations, Diverse Applications, and Research and Development (R&D) Opportunities.

The motivation for developing Ni-Mg-Co ferrite nanoparticles through the coprecipitation process is driven by the desire to create versatile, high-performance materials that are cost-effective, scalable, and environmentally sustainable, with broad applicability across various industries.

EXPERIMENTAL MATERIALS AND METHODS

The materials used in this synthesis include nickel nitrate hexahydrate ($Ni(NO_3)_2 \cdot 6H_2O$), magnesium nitrate hexahydrate ($Mg(NO_3)_2 \cdot 6H_2O$), cobalt nitrate hexahydrate ($Co(NO_3)_2 \cdot 6H_2O$), iron nitrate nonahydrate ($Fe(NO_3)_3 \cdot 9H_2O$), citric acid, and sodium hydroxide, all sourced from Merck, Germany, with a purity of 99%.

The synthesis of nanoparticles was conducted in four steps. During these stages, the concentrations of the two substances were varied while the concentrations of the remaining materialsremained constant. The temperature and reaction time were fixed at 60 degrees Celsius and 15 minutes, respectively.

Experimental

To prepare the first sample ($NiCo_{0.5}Fe_2O_4$), nickel nitrate hexahydrate ($Ni(NO_3)_2 \cdot 6H_2O$), cobalt nitrate hexahydrate ($Co(NO_3)_2 \cdot 6H_2O$), and iron nitrate nonahydrate ($Fe(NO_3)_3 \cdot 9H_2O$) were dissolved in 50 mL of deionized (DI) water. The ingredients were thoroughly mixed and then placed on a magnetic stirrer heater. Next, 1.5 M citric acid was dissolved in 50 mL of water, and 5 mL of sodium hydroxide (NaOH) was added dropwise to the mixture. Care was taken to monitor the pH closely; when it reached 7, adding NaOH was slowed, as increasing alkalinity (OH^- concentration) accelerates the reaction. The pH was controlled using a pH meter until it transitioned from acidic to alkaline, stopping the addition of hydroxide when the pH reached 12. It is important to note that a brown precipitate begins to form upon adding NaOH. At this point, the magnet was removed from the mixture, and the magnetic stirrer was turned off. The precipitate was collected using filter paper. In the next step, the collected precipitate was placed in an oven for 24 hours at room temperature, followed by annealing in a furnace for 2 hours at 600 degrees Celsius. This sample is designated as M01. Samples M02, M03, and M04 were prepared according to the compositions listed in Table 1.

Table 1

Changes in the molar percentage of the samples $Mg_xNi_{1-x}Co_{0.5}Fe_2O_4$

Sample	X	Chemical	Mg	Ni	Co	Fe
M01	0.00	$Ni\ Co_{0.5}Fe_2O_4$	0.00	0.50	0.5	2
M02	0.33	$Mg_{0.33}\ Ni_{0.67}\ Co_{0.5}\ Fe_2O_4$	0.15	0.35	0.5	2
M03	0.66	$Mg_{0.66}\ Ni_{0.34}Co_{0.5}\ Fe_2O_4$	0.30	0.20	0.5	2
M04	0.99	$Mg_{0.99}\ Ni_{0.01}CoFe_2O_4$	0.45	0.05	0.5	2

Instruments

X-ray diffraction (XRD) analysis was conducted using a BRUKER Advance D8 diffractometer with CuKα radiation (λ = 1.5405 Å) at room temperature (RT). The scans were performed over a 2θ° range from 5° to 75° with a step size of 0.020° and a scan step time of 1 second for structural analysis.

Morphological analysis was conducted using scanning electron microscopy (SEM, EM8000M-KYKY). The spectral analysis of all samples was performed using Fourier transform infrared (FT-IR) spectroscopy (BRUKER, TENSOR II). All instruments are in the Central Research Laboratory at the University of Sistan and Baluchestan, I. R. of Iran.

The magnetic properties of the samples were measured using a vibrating sample magnetometer (VSM, 7407 Lake Shore) at room temperature, located at Birjand University, I.R. of Iran.

RESULTS AND DISCUSSION:

X-ray diffraction (XRD) Analysis

After preparing the samples using the chemical co-precipitation method, X-ray diffraction (XRD) spectra were obtained to determine the type of synthesized crystal structure, the size of the crystallites (D), the average crystallite size, and the full width at half maximum (FWHM, β) of the diffraction peaks. The crystallite size (D) of the samples was calculated using Debye-Scherrer's formula:

$$D = (0.9\lambda/\beta cos\theta) \quad (1)$$

The average crystallite size was calculated and is presented in Table 2. The average size of the crystallites increased from M01 to M03 and then decreased for M04. The XRD data were analyzed using X'pert software to determine the phases and structures of the samples.

According to Figure 1 for sample M01, the presence of nickel, cobalt, and iron was noted in the formation of cobalt iron oxide ($CoFe_2O_4$, cubic structure with a = b = c = 8.390 Å), nickel ferrite ($NiFe_2O_4$), and iron oxide (magnetite, Fe_3O_4) at diffraction angles of 30.1°, 35.5°, 43.2°, 53.5°, 56.8°, and 62.8°.

Additionally, for sample M02, magnesium oxide (MgO), cobalt ferrite ($CoFe_2O_4$, cubic structure with a = b = c = 8.390 Å, at angles of 18.3°, 23.2°, 37.2°, 44.1°, 53.5°, 57.0°, and 62.5°), and magnesioferrite ($MgFe_2O_4$, at angles of 18.2°, 30.1°, 35.3°, 37.1°, 43.1°, 53.2°, 56.9°, and 62.2°) were observed.

Sample M03 exhibited characteristics similar to those of sample M02. In sample M04, cobalt oxide (CoO), iron oxide (Fe_2O_3), magnesioferrite ($MgFe_2O_4$, cubic structure with a = b = c = 8.397 Å), and magnesium oxide (MgO) were identified. A summary of the different phases is presented in Table 3.

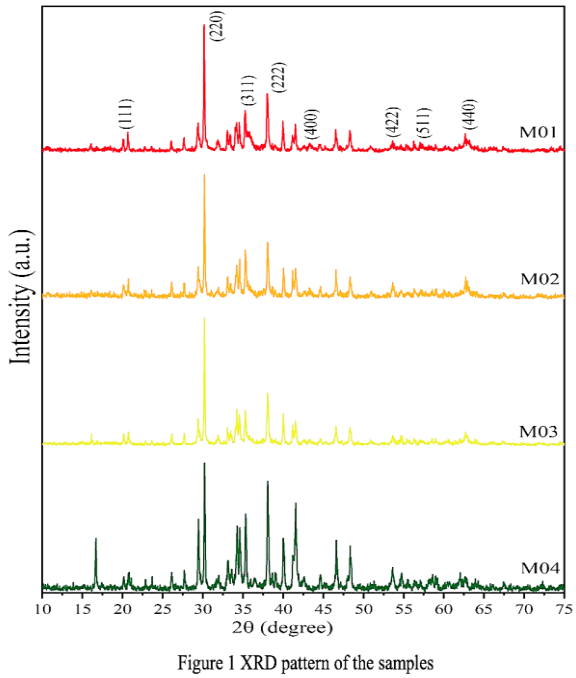


Fig. 1. XRD pattern of the samples

In all the samples, the compounds CoO and Fe_2O_3 exhibit a simple cubic (SC) crystal structure. Additionally, for samples M01 to M03, the composition of $NiFe_2O_4$ is also observed in an SC form. In M02 to M04 samples, the compositions of $CoFe_2O_4$, $MgFe_2O_4$, and MgO are similarly identified in SC form.

The diffraction peaks in the XRD patterns correspond to the crystal planes of the cubic spinel structures, specifically the (111), (220), (311), (222), (400), (422), (333), (511), and (440) faces. All these planes belong to the cubic spinel structure with the Fd3m space group. The diffraction peaks align well with those reported in the study by Kokare et al. [18].

Table 2
Average size of crystallites (nm)

Sample	M01	M02	M03	M04
Average size of crystallites (nm)	31.574	57.430	66.394	63.489

Table 3
Different Phases and $2\theta°$

Phases	2θ°
Fe_2O_3	18, 30.5, 36, 49, 62.5
MgO	36, 54
$CoFe_2O_4$, Cubic	18.3, 23.2, 37.2, 44.1, 53.5, 57.0, 62.5
Fe_3O_4	30.1, 35.5, 43.2, 53.5, 56.8, 62.8
$NiFe_2O_4$	18, 33.5, 41, 54
$MgFe_2O_4$	18.2, 30.1, 35.3,37.1, 43.1, 53.2, 56.9, 62.2

Zhao et al. [16] presented energy-dispersive X-ray spectroscopy (EDS) results for similar composites, identifying the main elements in their pure $Ni_{0.2}Mg_{0.2}Co_{0.6}Fe_2O_4$ nanoparticles as Ni, Mg, Co, Fe, and O. All prepared samples contained the same elements. EDS analysis confirmed the peaks corresponding to these elements in the synthesized samples, indicating that the ferrite samples possessed a pure phase and structure.

Spectral Analysis

Fourier transform infrared (FTIR) spectroscopy was conducted on the obtained samples for further investigation, as shown in Figure 2. The absorption peaks associated with the functional groups Fe-O, Co-O, Ni-O, and Mg-O overlap in the 400 to 700 cm^{-1} frequency range. In sample M01, absorptions for the Fe-O, Ni-O, and Co-O functional groups were observed. In samples M02 and M03, absorptions were detected for Fe-O, Ni-O, Co-O, and Mg-O, while sample M04 exhibited absorptions for Fe-O, Co-O, and Mg-O.

Additionally, a characteristic peak resembling a "W" shape in all samples within the frequency range of 1400 cm^{-1} indicates the presence of the O-H functional group. Furthermore, a distinct curve in sample M04 in the frequency range of 2600 to 3600 cm^{-1} suggests the presence of the Mg-O functional group in its structure.

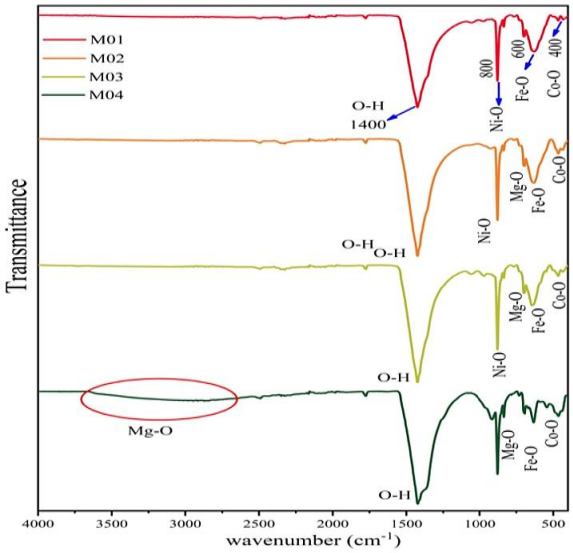
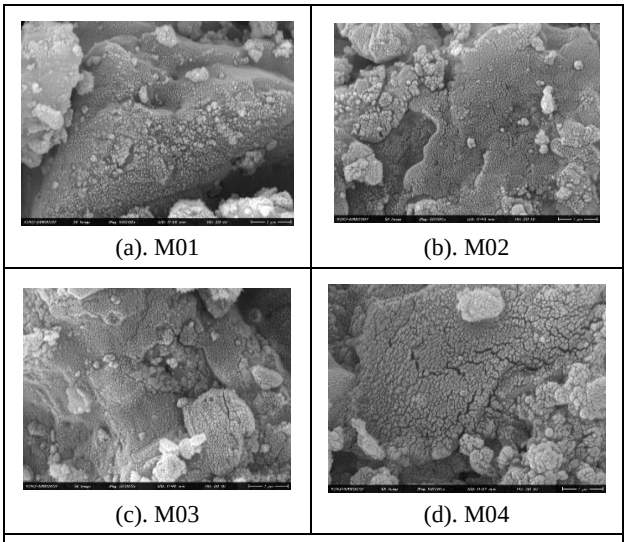


Fig. 2. FTIR spectra of the samples

Morphological Analysis

Scanning electron microscopy (SEM) has been used at magnification 50000 for detailed examination of the surface structures. Figures 3(a-d) presented the SEM nanostructure of the samples before (M01) and after adding magnesium (M02, M03, M04). The surface morphology of the samples possesses spherically shaped grain with good homogeneity, as shown in Fig. 3(b-d).



(a). M01 (b). M02

(c). M03 (d). M04

Fig. 3. (a). SEM Image of: (a). M01 without Magnesium, and (b). M02, (c). M03, (d). M04 with Mg

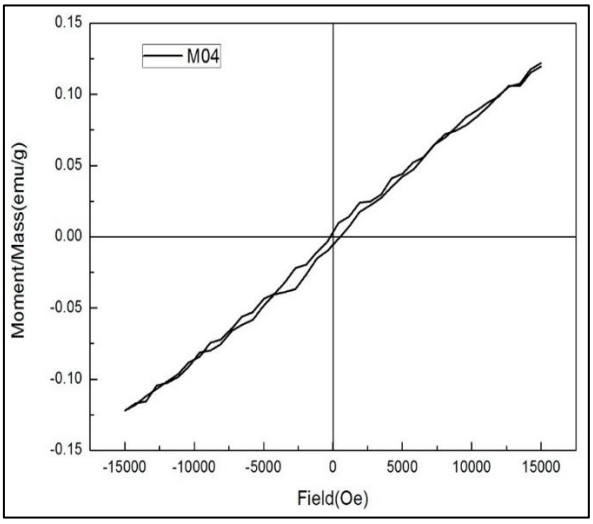


Fig. 5. M-H hysteresis of the M04 sample

Magnetization Investigation

According to Figure 4 and Table 4 show that the values of saturation magnetization (M_s) and remanent magnetization (M_r) decrease with increasing Mg content. This reduction may be attributed to the lower nickel content in sample M04. The samples M01, M02, and M03 exhibit ferromagnetic properties, with sample M02 demonstrating a harder ferromagnetic behavior than the other samples. In contrast, sample M04 displays characteristics similar to paramagnetism.

The square (M_r/M_S) needs to be large to help reduce the demagnetization effect of itself and improve the information recording effect [16]. In this work M_r/M_S for M01 and M02 increase and then for M03 and M04 decrease.

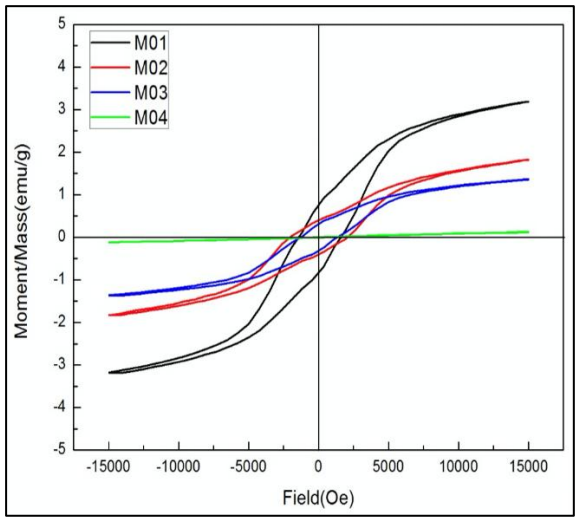


Fig. 4. Magnetic hysteresis loops of the samples

Information regarding the magnetic properties of the samples is provided in Table 4. The decreasing values in saturation magnetization of the samples M01-M04 may be due to the presence of impurity phase of Fe_3O_4 (Magnetite) that was observed in the XRD pattern. The appearance of the weakly magnetic, impure phase of Fe_3O_4 (Magnetite) can reduce the saturation magnetization.

It is well known that the magnetic properties of ferrites with the AB_2O_4 spinel crystal structure depended on the composition of cation in tetrahedral A site and octahedral B site. A decrease in M_S is expected when the Mg^{2+} is added to the ferrite lattice. Since paramagnetic Mg^{2+} is known to occupy the octahedral B sites and reduce the density of the magnetic ions in B-sublattice, thus reducing not only the magnetic moment of the sublattice but also the exchange interaction.

Table 4
Magnetic parameters of the samples

Sample	Remanent Magnetization (M_r) emu/g	Saturation Magnetization (M_s) emu/g	Coercivity (H_c) Oe	Squareness (S) M_r/M_s
M01	0.54	3.19	254.76	0.168
M02	0.32	1.83	432.40	0.174
M03	0.21	1.37	221.49	0.157
M04	4.32×10^{-3}	0.12	339.15	0.035

CONCLUSION

In this research, the synthesis of tetra metallic nanocomposite (nickel-magnesium-cobalt-ferrite) was successfully achieved using the co-precipitation method. Four samples were prepared: M01, which lacked magnesium, and M02, M03, and M04, which contained all four elements, with M04 exhibiting almost negligible nickel content. The samples underwent X-ray diffraction (XRD), scanning electron microscopy (SEM), and vibrating sample magnetometry (VSM) to evaluate their structural and magnetic properties.

XRD analysis revealed that all samples exhibited metal oxides and ferrites in a simple cubic crystal structure. Notably, the average crystal size increased by adding magnesium up to M04. Fourier transform infrared spectroscopy (FTIR) confirmed the presence of expected chemical bonds. SEM images indicated that the nanostructures were cubic and displayed a cauliflower-like morphology with a uniform dispersion of metal ferrites.

VSM results demonstrated that samples M01, M02, and M03 exhibited ferromagnetic characteristics, with M02 displaying hard ferromagnetic behavior, while M04 showed properties like paramagnetism. The incorporation of magnesium and the reduction of nickel led to a decrease in saturation magnetization from 3.19 to 0.12 emu/g, alongside a reduction in residual magnetization from 0.54 to 4.32×10^{-3}.

The future outlook for Ni-Mg-Co ferrite nanoparticles synthesized via the co-precipitation method appears promising, particularly in magnetics, catalysis and biomedicine applications. Ongoing research may explore several strategies to enhance the performance of these nanoparticles, including: Doping with Other Elements, Surface Functionalization, Size and Morphology Control, Composite Formation, Magnetic Field Applications, Sustainability and Biodegradability

These approaches could significantly broaden the applicability and efficiency of Ni-Mg-Co ferrite nanoparticles in various advanced technological fields.

By focusing on these modification strategies, researchers can enhance the performance of Ni-Mg-Co ferrite nanoparticles, broadening their applicability in advanced technologies and addressing current limitations.

ACKNOWLEDGEMENTS:

Authors sincerely thank the cooperation of the Research Vice-Chancellor of the University of Sistan and Baluchestan. I. R. of IRAN.

CONFLICTS OF INTEREST

The authors declare that there are not conflicts of interest regarding this article.

REFERENCES

[1] Kefeni KK, Msagati TA, Nkambule TT, Mamba BB. Spinel ferrite nanoparticles and nanocomposites for biomedical applications and their toxicity. Mater Sci Eng C. 2020;107:110314.

[2] Hu J, Ma Y, Kan X, Liu C, Zhang X, Rao R, Zheng G. Investigations of Co substitution on the structural and magnetic properties of NiZn spinel ferrite. J Magn Magn Mater. 2020;510:166940.

[3] Gao JM, Li W, Ma S, Du Z, Cheng F. Spinel ferrite transformation for enhanced upgrading nickel grade in laterite ore of various types. Miner Eng. 2021;168:106908.

[4] Angotzi MS, Mameli V, Cara C, Musinu A, Sangregorio C, Niznansky D, Cannas C. Coupled hard–soft spinel ferrite-based core–shell nanoarchitectures: magnetic properties and heating abilities. Nanoscale Adv. 2020;2(5):2034-2043.

[5] Jalili H, Aslibeiki B, Eskandarzadeh N. Advanced applications of spinel ferrite nanoparticles in medicine: Magnetic hyperthermia, magnetic resonance imaging and targeted drug delivery. Iran J Phys Res. 2021;21(1):31-39.

[6] Pham TN, Huy TQ, Le AT. Spinel ferrite (AFe2O4)-based heterostructured designs for lithium-ion battery, environmental monitoring, and biomedical applications. RSC Adv. 2020;10(52):31647-31674.

[7] Tian Y, Shao X, Zhu M, Liu W, Wei Z, Chu K. A spinel ferrite catalyst for efficient electroreduction of dinitrogen to ammonia. Dalton Trans. 2020;49(36):12733-12740.

[8] Deepty M, Ch S, Ramesh PN, Mohan NK, Singh MS, Prajapat CL, Sastry DL. Evaluation of structural and dielectric properties of Mn2+-substituted Zn-spinel ferrite nanoparticles for gas sensor applications. Sens Actuators B Chem. 2020;308:127716.

[9] Bhandare SV, Kumar R, Anupama AV, Choudhary HK, Jali VM, Sahoo B. Mechanistic insights into the sol-gel synthesis of complex (quaternary) Co–Mn–Zn-spinel ferrites: An annealing dependent study. Ceram Int. 2020;46(18):28619-28630.

[10] Phor L, Chahal S, Kumar V. Zn2+ substituted superparamagnetic MgFe2O4 spinel-ferrites: Investigations on structural and spin-interactions. J Adv Ceram. 2020;9(3):374-386.

[11] Shao L, Sun A, Zhang Y, Yu L, Zuo Z, Suo N. Cr3+-doped nanocrystalline nickel–magnesium–cobalt spinel ferrite: microstructural and magnetic properties. Appl Phys A. 2021;127(1):48.

[12] Zuo Z, Sun A, Yu L, Suo N, Zhang W, Zhao X. Study on structure and magnetic properties of Cr3+-doped Ni–Cu–Co ferrites prepared by sol–gel method. Mod Phys Lett B. 2020;34(33):2050325.

[13] Yu L, Sun A, Suo N, Zuo Z, Zhao X, Zhang W, Zhang Y. Enhancement of magnetic properties of Ni–Mg–Co ferrites by Y3+ ions doping. J Mater Sci Mater Electron. 2020;31(11):8600-8609.

[14] Ling C, Wang Z, Ni Y, Zhu Z, Cheng Z, Liu R. Superior adsorption of methyl blue on magnetic Ni-Mg-Co ferrites: Adsorption electrochemical properties and adsorption characteristics. Environ Prog Sustain Energy. 2020;39(5):e13367.

[15] Suo N, Sun A, Yu L, Zuo Z, Zhao X, Zhang W, Dang Z. Effect of Al3+ ion-substituted Ni–Mg–Co ferrite prepared by sol–gel auto-combustion on lattice structure and magnetic properties. Appl Phys A. 2020;126(6):450.

[16] Zhao X, Sun A, Zhang W, Yu L, Zuo Z, Suo N, Han Y. Studies on structural and magnetic properties of Ni-Mg-Co spinel ferrite nanoparticles sintered at different temperatures. Mod Phys Lett B.

2020;34(5):2050052.

[17] Zhao X, Sun A, Zhang W, Han Y, Pan X. Effects of Mg substitution on the structural and magnetic properties of Ni0.2MgxCo0.8−xFe2O4 nanoparticle ferrites. J Supercond Nov Magn. 2019;32(4):1037-1045.

[18] Kokare MK, Jadhav NA, Kumar Y, Jadhav KM, Rathod SM. Effect of Nd3+ doping on structural and magnetic properties of Ni0.5Co0.5Fe2O4 nanocrystalline ferrites synthesized by sol-gel auto combustion method. J Alloys Compd. 2018;748:1053-1061.